SUPPLEMENTARY MATERIAL

Text S1. GLS recording schedule.

The models of GLS used in this study measure light levels, within a range of light intensities associated with twilights (i.e., dim lights); electrical conductance between two electrodes, a proxy for saltwater immersion, and therefore, for the at-sea activity of the birds; and the temperature when immersed (Biotrack Ltd. 2013). Every 10 min the GLS store the highest light intensity (measured on an arbitrary scale between 0 and 64) recorded in the previous 10 min. The immersion was measured every 3 s (dry = 0, wet = 1), and every 10 min the immersion values were summed (0 to 200). Mk7 GLS models recorded the exact time of transitions between wet and dry (measured every 3 s) which resulted in the memory filling up quicker. The GLS measured the temperature only when immersed and stored it only after 20 min of continuous immersion, the recording schedule when wet for more than 20 min varied slightly across models (Biotrack Ltd. 2013).

Text S2. On-bird calibration

The determination of the zenith angle corresponding to the chosen threshold is ideally done by "roof-top calibration" before or after deployment (Lisovski et al. 2012b). Unfortunately, the length of pre-deployment calibration was not long enough to reliably estimate the zenith angle. Instead, the zenith angles were determined using on-bird calibration whilst the birds were on Christmas Island, which may be less ideal as the behaviour of the animals at twilight might affect the calibration (Hill & Braun 2001, Lisovski et al. 2012b). To assess the viability of the following on-bird calibration method as replacement for the more standard roof-top calibration, both methods were used on the stationary GLS left on Christmas Island for 10 months (GLS model Mk4). Calibration values obtained from the roof-top calibration of the stationary GLS were then used to estimate locations for deployed GLS of the same model (n = 3), and results were compared with locations obtained with individual GLS on-bird calibration. Results supported the use of on-bird calibration as a viable alternative to roof-top calibration for this study (for details see Text S2).

As the nest sites were only monitored once or twice annually between August and October, three criteria were used to support the assumption that the birds were on or close to Christmas Island during the period used for on-bird calibration. Two out of the three following criteria had to be met for a period to be considered for on-bird calibration. (1) The bird was sighted on the island during this period. (2) The light data did not deviate much from the corresponding estimated twilight on Christmas Island (Figure S6, a) and showed little light interference, i.e., it was likely to be bound to Christmas Island but unlikely to be incubating or brooding. (3) When activity data were available, the night immersion was extremely low (i.e., mostly full "dry" nights; Figure S6, b). In combination with criterion two, this indicates the bird was more likely to be spending the night on Christmas Island rather than being out at sea, hence it is more likely that it was already back on the island at twilight, or at least close to the island. Twilights associated with "wet" nights were removed for the calibration to limit the influence of outliers as the bird was likely to be out at sea for at least part of the night. When no such period could be defined for a GLS, the average calibration parameters from other GLS of the same model were used for the estimation of locations.

Once the on-bird calibration period had been defined, the most appropriate threshold was determined by computing for that period the mean squared error (MSE) of the latitude difference between the location estimates and Christmas Island for a range of thresholds. For each threshold the MSE was calculated for a range of zenith angles to assess the effect of threshold/zenith angle mismatch (Hill & Braun 2001, Lisovski et al. 2012b) and find which threshold resulted in the lowest MSE (Figure S7). The median "best" threshold per model was used for further processing (for Mk4 and Mk7 it was 2.5; for Mk15 and Mk3006 it was 1.0). The corresponding zenith angle was defined by computing for the full deployment period the location estimates at a range of different zenith angles with a simple threshold method and following the criteria defined by Bråthen et al. (2021). The resulting paths were mapped (Figure S8) and the latitudes plotted over time (Figure S9). As the effect of a threshold/zenith angle mismatch is inversed on either side of an equinox (Figure S9; Hill & Braun 2001, Lisovski et al. 2012b), the most appropriate zenith angle was defined as (1) resulting in the most concentrated cluster of locations around Christmas Island for the period where the raw light data indicated that they spent most of their time, and (2) having the latitudes on either side of an equinox as close as possible to Christmas Island (apart from the periods where the light data deviated significantly from twilight at Christmas Island).

Text S3. Assessment of on-bird calibration as an alternative to roof-top calibration.

To assess the viability of the on-bird calibration method detailed in this study as replacement for the more standard roof-top calibration, both methods were used on the stationary GLS left on Christmas Island for 10 months (GLS model Mk4). Calibration values (zenith angle, zenith zero deviation, and twilight error distribution) obtained from the roof-top calibration of the stationary GLS were then used to estimate locations for deployed GLS of the same model (n = 3), and results were compared with locations obtained with individual GLS on-bird calibration.

The 'best' threshold for the stationary GLS was identified using the same procedure as on-bird calibration, i.e., by plotting the mean squared error (MSE) of latitude difference with Christmas Island outside of an equinox period (i.e., 21 days either side of an equinox) for location estimates obtained using the simple threshold method at a range of different thresholds and different zenith angles, and retrieving the threshold that resulted in the minimum MSE. While the overall minimum MSE was obtained at a threshold of 10 (MSE = 5.23), minimum MSE for thresholds of 5 and 2.5 were comparable (5.38 and 5.36, respectively) (Figure S11). Therefore, a threshold of 2.5 was retained for further processing to allow comparison with other Mk4 GLS deployed on birds for which the median 'best' threshold was identified as 2.5 (see Text S2). The more standard roof-top calibration was then performed using the function thresholdCalibration in the package TwGeos which returns the zenith angle (z = 97.1), zenith zero deviation (z0 = 99.6), and the twilight error distribution (gamma distribution with shape = 5.69, and scale = 0.56). The on-bird calibration method detailed in this study (see Texts S2 and S3) was followed to retrieve a second set of zenith angle (z = 96.8) and zenith zero deviation (z0 = 98.9), to use along with a generic twilight error distribution for open habitat species (log normal distribution with 'shape' ($\log(\mu)$) = 2.49, and 'scale' ($\log(\sigma^2)$) = 0.94; Merkel et al. 2016). The package SGAT was used to refine the locations with both sets of calibration values following the method detailed in this study (see Text S4). Equinox periods were removed, and the mean distance between the locations and Christmas Island was

calculated, both with a single fixed latitude and with a single fixed longitude to assess the effect of the different sets of calibration values on the latitudinal and longitudinal accuracy of the location estimates.

The mean latitudinal distance between location estimates and Christmas Island using the roof-top calibration values was 242 ± 155 km (mean ± SD), and for location estimates obtained using the on-bird calibration values and the generic distribution it was 356 ± 227 km. Mean longitudinal distance with roof-top calibration values was 68 ± 50 km, and for on-bird calibration 64 ± 45 km. While the on-bird calibration resulted in lower latitudinal accuracy it remains comparable to average GLS accuracy (304 ± 413 km with the package probGLS and 408 ± 473 km with the package flightR; Halpin et al. 2021). Longitudinal accuracy was unaffected.

Next, location estimates for Mk4 GLS deployed on birds were obtained using (1) the values from the stationary GLS roof-top calibration (z = 97.1; z0 = 99.6; gamma distribution with shape = 5.69, and scale = 0.56), and (2) values from on-bird calibration determined individually for each deployed GLS. Locations were refined with the package SGAT following the procedure mentioned in this study (see Text 3). To compare the results, maps of the tracks were produced (Figure S12), and latitude plotted over time (Figure S13). Additionally, the net squared displacement (NSD) was calculated and plotted over time (Figure S14). Results were compared visually.

Overall, location estimates seem more plausible with individual GLS on-bird calibration. Latitudinal peaks of locations during the equinox can be a symptom of poorly calibrated data (Lisovski et al. 2012b). Estimation of locations with on-bird calibration values resulted in less latitudinally spread-out locations (Figures S12, S13), particularly around the equinox (Figures S13, S14), than when locations were estimated with roof-top calibration values from the stationary GLS. A latitudinal difference in the clustering of location estimates either side of an equinox (e.g., further North between March and September, and further South between September and March) for periods when birds are assumed to be bound to Christmas Island can result from a mismatch between the threshold and corresponding zenith used (Lisovski et al. 2012b). Apart from obvious deviations from the expected twilight on Christmas Island corresponding to non-breeding migrations (Figure S13 - G, H, I), the light data showed little deviation supporting the assumption that the birds did not undertake significant trips during most of the deployment period and were likely bound to Christmas Island. However, this segregated clustering pattern either side of an equinox can be observed for locations refined with roof-top calibration values from the stationary GLS (Figure S13 - A, B, C), less so for locations refined with individual GLS on-bird calibration (Figure S13 - D, E, F). These results support the use of on-bird calibration as a viable alternative to roof-top calibration in this study.

Text S4. Refinement of location estimates

The location estimates were refined using the R package SGAT (v0.1.3; Lisovski et al. 2012a, Sumner et al. 2009), a Bayesian framework that uses prior information on the species ecology to compute a posterior distribution of location estimates by Markov Chain Monte Carlo (MCMC). Speed and twilight error distributions, a land mask (0.25°x0.25° resolution), and the mean daily temperatures recorded by the loggers were used as priors (Lisovski et al. 2019). The initial path obtained from the simple threshold method served as starting point in

the first iteration of the MCMC. At each iteration, for each location estimate, a new location was sampled and its likelihood calculated. The speed prior distribution was obtained from previous GPS deployments on Abbott's boobies during early chick rearing (Hennicke & Weimerskirch 2014a). Following Hennicke and Weimerskirch (2014a), GPS speeds below 7 km h^{-1} were removed as they were considered to correspond to the birds being on water. Of the remaining data, 100 speed records were sampled per bird (n = 47) and a gamma distribution was fitted to the sampled data (Lisovski et al. 2019). This operation was repeated 1,000 times and the mean shape and rate of the speed gamma distributions was used as prior in the MCMC. This is a conservative speed prior as the birds are unlikely to be flying continuously in a straight line between two GLS locations (c. 12h). As the birds' behaviour during the on-bird calibration potentially affected the shape of the twilight error distribution (i.e., the difference between when twilights were recorded and when they actually occurred) a more generic distribution for open habitat species was used as prior (log normal distribution with 'shape' ($\log(\mu)$) = 2.49, and 'scale' ($\log(\sigma^2)$) = 0.94; Merkel et al. 2016). The largest zenith angle of the twilight error distribution, thereafter the zenith zero deviation (z0), serves as the starting point of the distribution. It was defined by plotting the light data during the on-bird calibration period against the zenith angle on Christmas Island when the light data were recorded using the function thresholdCalibrate in the package TwGeos (Figure S10). Isolated points corresponding to larger zenith angles than most of the other twilights were assumed to indicate that the birds where away from Christmas Island and, therefore, were not considered for the determination of the z0. NOAA Optimum Interpolation Sea Surface Temperature (SST) V2 at 1°x1° resolution (NOAA OI SST V2 High Resolution Dataset https://psl.noaa.gov accessed 21 Dec 2021) was used for the estimation of the posterior SST distribution. For Mk7 the temperature memory was saturated after about 3 months which did not cover fully any non-breeding periods. When the temperature was not available the MCMC only used the other priors. Locations were first refined using the Essie model (epsilon1 = $1.0e^{-4}$) which samples new locations on a lattice of grid points (Wotherspoon et al. 2021). It cannot capture small scale variations of likelihood for the posterior distribution of locations but quickly reaches general areas of high likelihood. Locations were further refined using Estelle model with first a burn-in period (1 chain, iterations = 1000, thinning = 60) to quickly get the locations to areas of high likelihood at a smaller scale, then a tuning period (chains = 2, iterations = 1000, thinning = 60) to ensure posterior distributions remain in areas of high likelihood, and a final run (chains = 4, iterations = 5000, thinning = 60). The final location estimates were calculated from the mean of posterior distributions of all iterations in the final run.

Text S5. Identification of migrations

The migrations were defined as periods when the birds were further than 500 km from Christmas Island (i.e., maximum known distance travelled by the adults during early chick rearing; Hennicke & Weimerskirch 2014b) for more than 14 continuous days (i.e., based on the expected maximum duration between two attendances of the chick; Nelson & Powell 1986). To identify these periods in a repeatable and robust way, and resolve uncertainties during the equinox period, we used visual inspection of two metrics - the net squared displacement from Christmas Island (NSD), and the squared longitude difference (i.e., between the location estimates and Christmas Island, SLD) (Figure S15). The departure and return dates were defined, respectively, as the latest and earliest date when the NSD was virtually undistinguishable from 0 (i.e., on Christmas Island), before / after the NSD intersected the 500 km threshold (Figure S15). The end of the migration was often within the equinox

period. In such cases, the NSD was not reliable to identify the return date. Instead, as the migrations were mostly longitudinal (see "results") and the longitude is largely unaffected around the equinox, the return dates within an equinox period were identified using the SLD. For five birds, two complete migrations were recorded. In total, 6,906 location estimates were retained (242 ± 53 per bird for full migrations) for a total of 27 full and 2 incomplete migrations.

Text S6. Determination of the phenophases

The phenophases were determined using the standard squared displacement method (Börger & Fryxell 2012), using the double-sigmoid model for the migration data (Bunnefeld et al. 2011) applied to mean squared displacement data (MSD, average per day) using non-linear mixed effects models (Börger & Fryxell 2012), with Christmas Island as the day zero start point. Models were fitted in R using the nlme package (v3.1.152; Pinheiro et al. 2021) and the concordance criterion to assess model fit (Börger & Fryxell 2012). Using the double-sigmoid migration model, the end of the outward migration was defined as the time when the individuals had reached within 5% of the asymptotic distance, identified as the estimated inflexion point parameter plus three times the estimated scale parameter (Figure S16; Börger & Fryxell 2012). For two individuals there was not one single non-breeding area, instead the individuals shifted to a second range. In order to quantify appropriately both movements, this was modelled as two outwards movements, and as one single return movement, using the single-sigmoid model (Börger & Fryxell 2012). For one track, the double-sigmoid model did not fit as the bird moved consistently away from Christmas Island over several weeks and returned to the island within only a few days. The end of the outbound migration/start of the return migration was therefore determined visually from the MSD. Two trips were incomplete, as the loggers stopped recording before the return trip. These two incomplete trips were fitted using the single-sigmoid MSD model and only the outbound migration was retained for analyses involving the phenophases.

Text S7. Estimation of breeding success

The outcome of the breeding attempt preceding a migration was estimated primarily from the data on the breeding status recorded during annual field surveys using criteria based on the species breeding biology (Nelson & Powell 1986), in particular the stage at which the devices were deployed (i.e., on an egg or with a young chick) in relation to the length of the breeding cycle (c. 17 months from pairing to the final departure of the chick). Criteria were; (1) if the bird undertook a migration in the same year as the deployment (determined from the tracking data) or within a year from an incubation period (determined from the light data) it was considered failed (n = 16); (2) if a year after deployment the tagged bird was observed involved in a new breeding attempt the previous one was considered failed (n = 2); (3) if a year after deployment a fledgling was seen at the nest site, the attempt was considered most likely to have subsequently succeeded (n = 3); (4) if a year after deployment the nest site still showed signs of activity (e.g., guano), but not associated with a new breeding attempt (e.g., new nest, adult on nest), it was considered most likely to come from a free flying fledgling still visiting the nest site and therefore successful (n = 4); (5) if none of the previous criteria applied the outcome of the breeding attempt was considered unknown (n = 4). Note that these estimations are liable to overestimation of the number of successful breeding attempts and underestimation of the failed ones, therefore, results must be interpreted with caution.

Text S8. Calculation of utilisation distributions

Utilisation distributions (UDs) were calculated using fixed kernel density estimation (Fieberg & Borger 2012, Horne et al. 2020) on a 50 x 50 km grid (Clay et al. 2017) with R package adehabitatHR (v0.4.19; Calenge 2006). The 99.9%, 95%, and 50% UDs were used to quantify the full range (99.9%), and to derive measures as used in standard seabird conservation mapping literature (95% home range and 50% 'core area') (e.g., Fromant et al. 2020, Hipfner et al. 2020, Börger 2021). A bandwidth of 186 km was used following Lascelles et al. (2016) which is based on the assessment of geolocation accuracy from Phillips et al. (2004). Though more recent studies found a lower accuracy of light level geolocation (on average 304 ± 413 km with the package probGLS and 408 ± 473 km with the package flightR; Halpin et al. 2021), and the estimated accuracy for Abbott's boobies non-breeding migration is lower as well, the bandwidth is not directly related to the accuracy of the locations (Hines et al. 2005, Fieberg 2007). For the Abbott's booby tracking data, the standardized approach from Lascelles et al. (2016) was found to account for the uncertainty of the location estimates, i.e., the full range contour line was at least 400 km away from 99% of all locations; while minimizing over smoothing, i.e., it did not include too much land masses (9% of 99.9% UD area on land). To account for different trip durations and number of trips per bird for the estimation of the population-level non-breeding range, UDs were first calculated per trip, then averaged per individual for each grid cell, and finally averaged across individuals.

Text S9. Sampling of pseudo-absence locations for habitat preference

Pseudo-absence locations were sampled by computing correlated random walks (CRW) with a land mask (R package SiMRiv; Quaglietta & Porto 2023). The parameters for the CRW (i.e., dispersion parameter of the turning angles, step length) were obtained from the observed tracks. The appropriate number of pseudo-absence locations was determined by measuring changes in χ^2 values (Clay et al. 2017, Žydelis et al. 2011). For each variable the binomial GAMM was run with increasing number of CRW and the χ^2 value recorded. For all variables the χ^2 value had stabilised by 70-80 (Figure S17). Therefore, for each observed track, 80 CRWs were generated and given the timestamps and bird identity of the observed track.

FIGURES

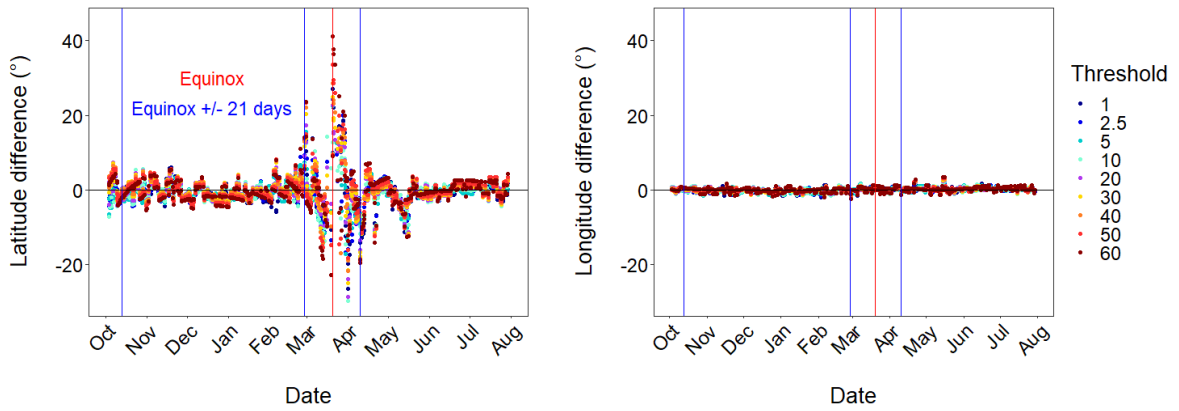

Figure S1. Latitude and longitude difference between location estimates (simple threshold method) and Christmas Island over time for the stationary GLS left 10 months on the island.

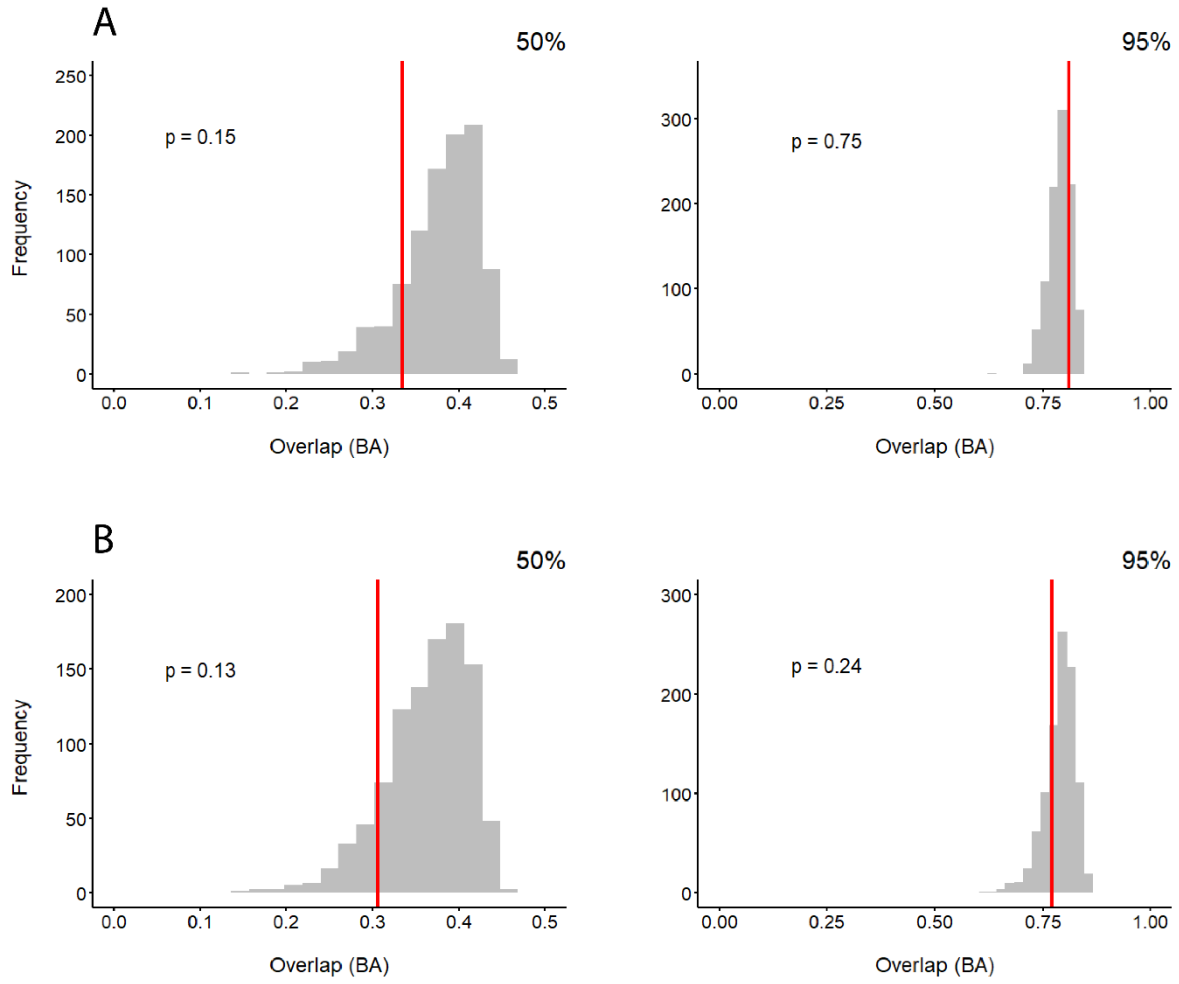

Figure S2. Observed overlap (red line; Bhattacharyya's affinity index) between (A) males and females, (B) failed and successful breeders, compared to the overlaps from the randomisation procedure (histogram, n=1000) for the 50% and 95% UDs.

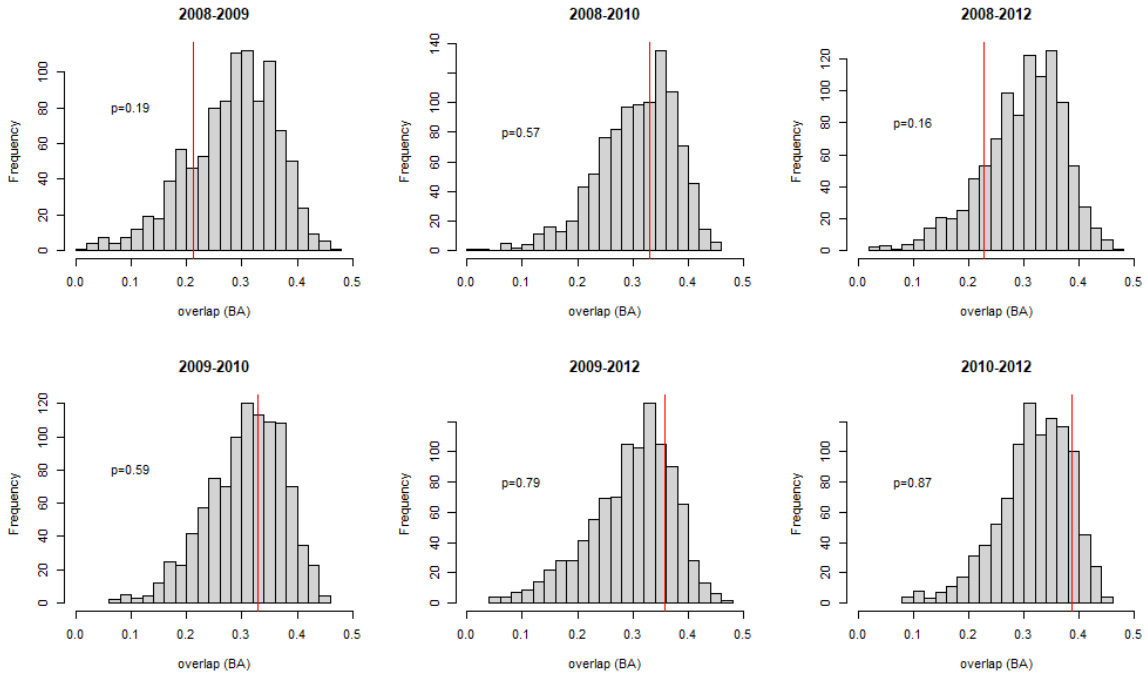

Figure S3. Observed overlap (red line, Bhattacharyya's affinity index, BA) between years, compared to the overlaps from the randomisation procedure (histogram, n=1000) for the core area (50% UDs).

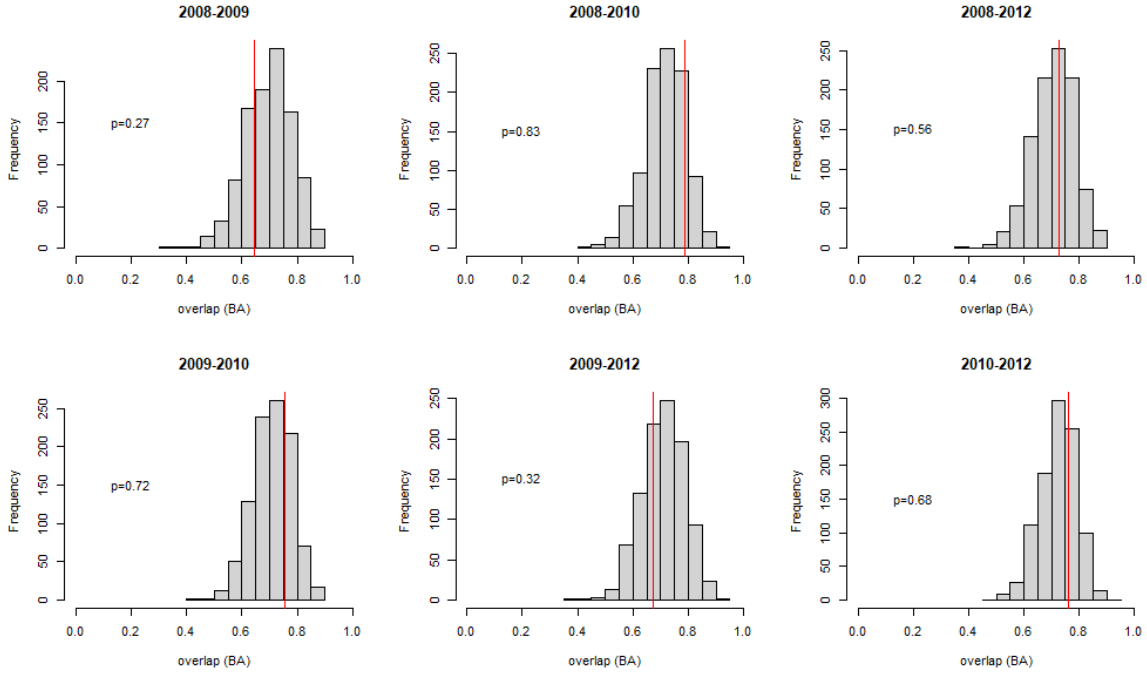

Figure S4. Observed overlap (red line, Bhattacharyya's affinity index, BA) between years, compared to the overlaps from the randomisation procedure (histogram, n=1000) for the home range (95% UDs).

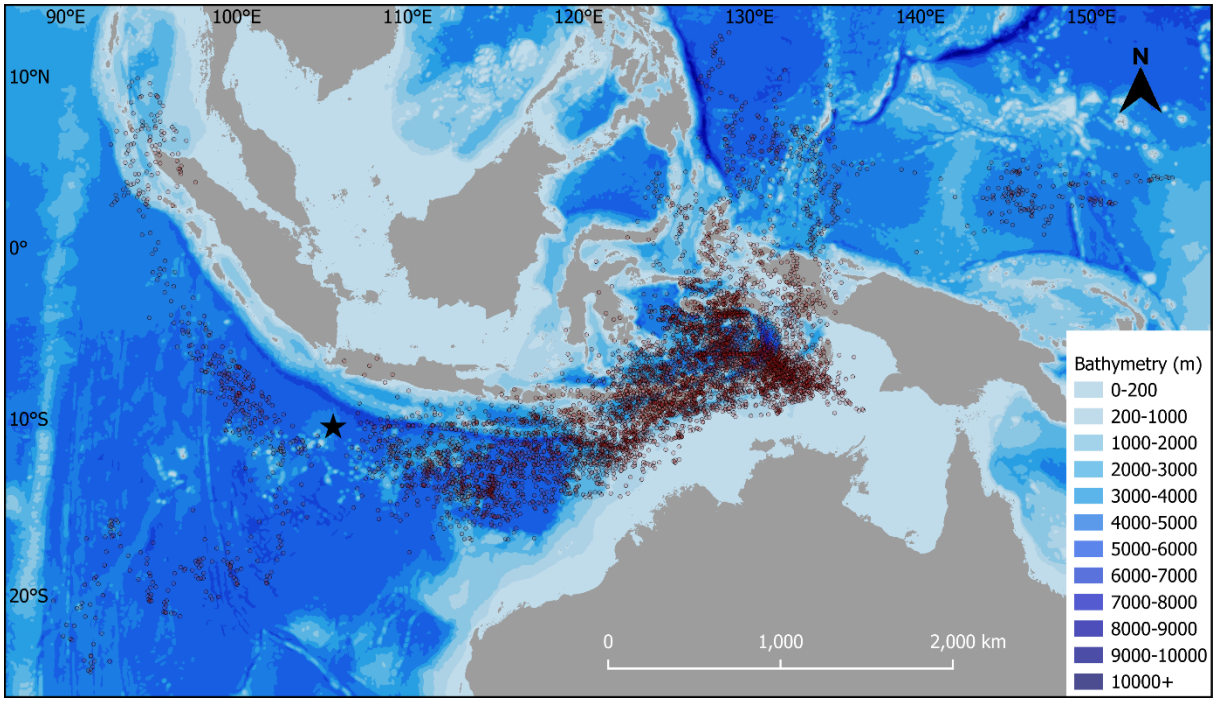

Figure S5. Distribution of location estimates from this study in relation to the bathymetry (m). Star = Christmas Island.

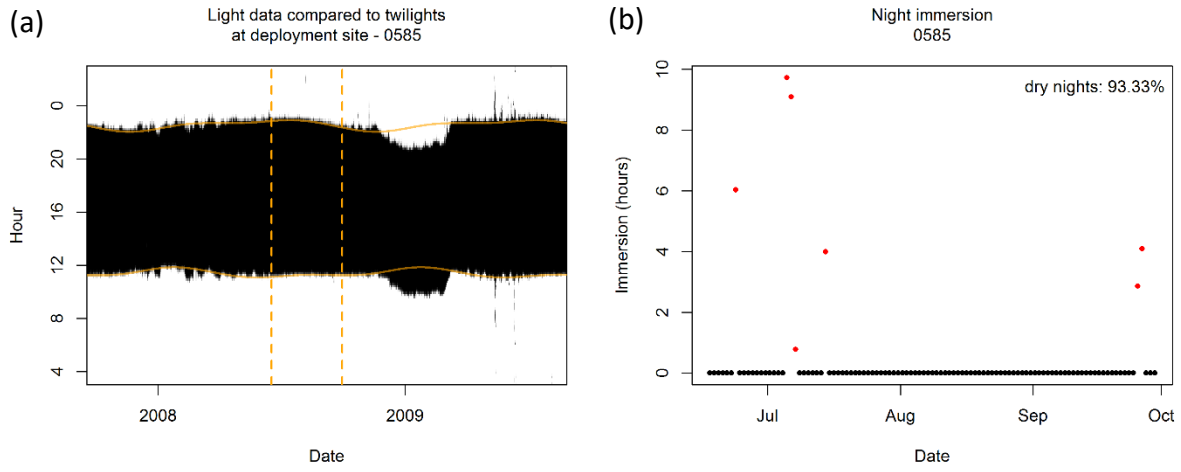

Figure S6. Example of light and immersion data used to identify suitable on-bird calibration period. (a) Continuous orange lines: twilight events on Christmas Island. Vertical dashed orange lines: boundaries of potential period for on-bird calibration. (b) The night immersion plot corresponding to the potential period for on-bird calibration.

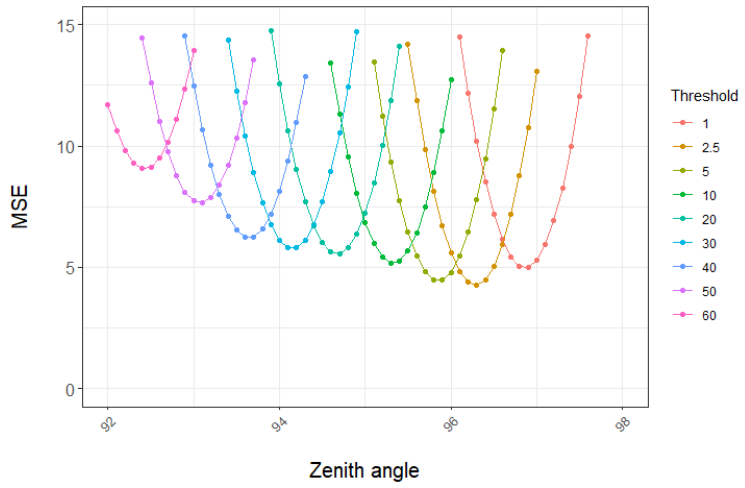

Figure S7. Mean squared error (MSE) of latitude difference between location estimates and Christmas Island during on-bird calibration period for an example GLS.

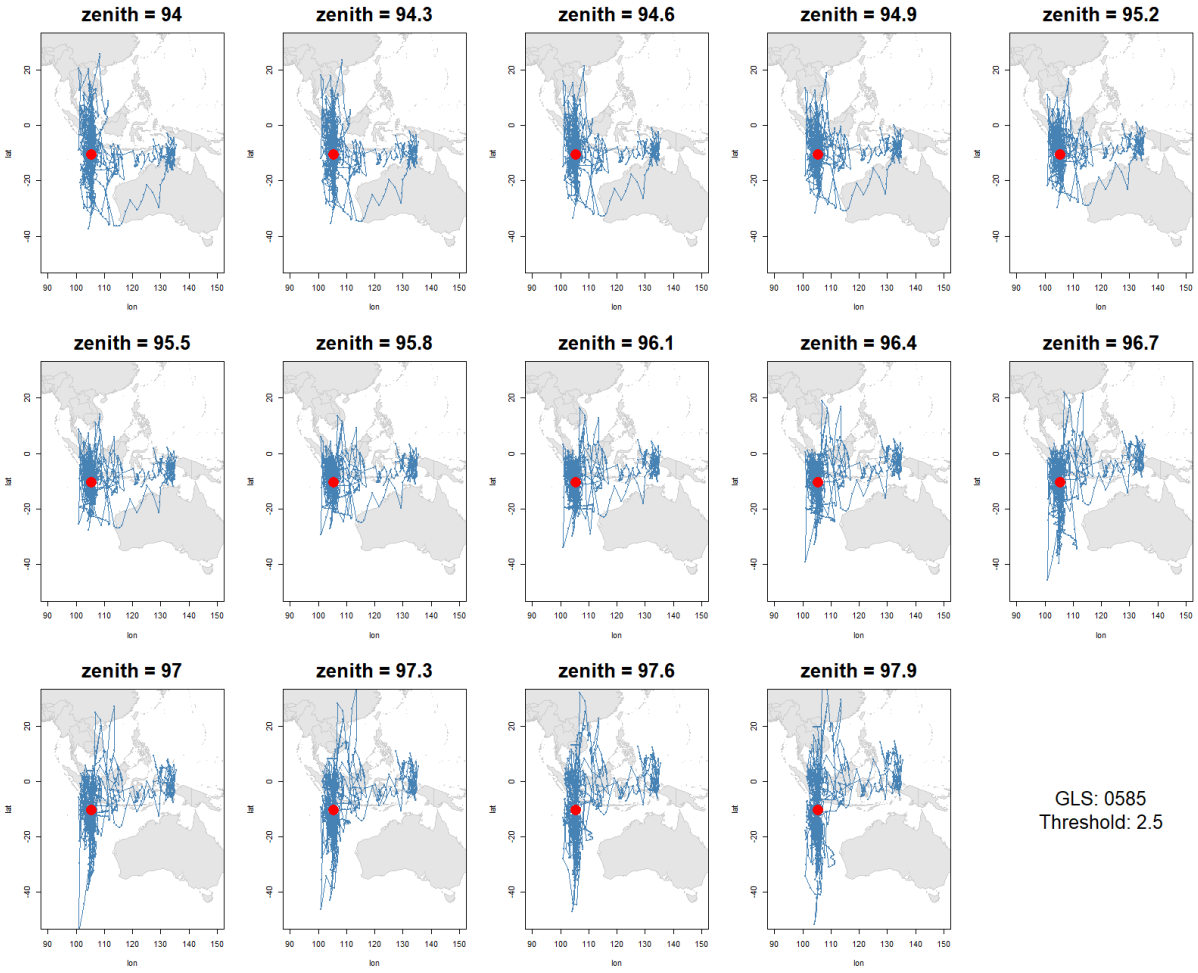

Figure S8. Track of raw location estimates (simple threshold method) at different zenith angles for the full deployment period of an example GLS. Red dot: Christmas Island.

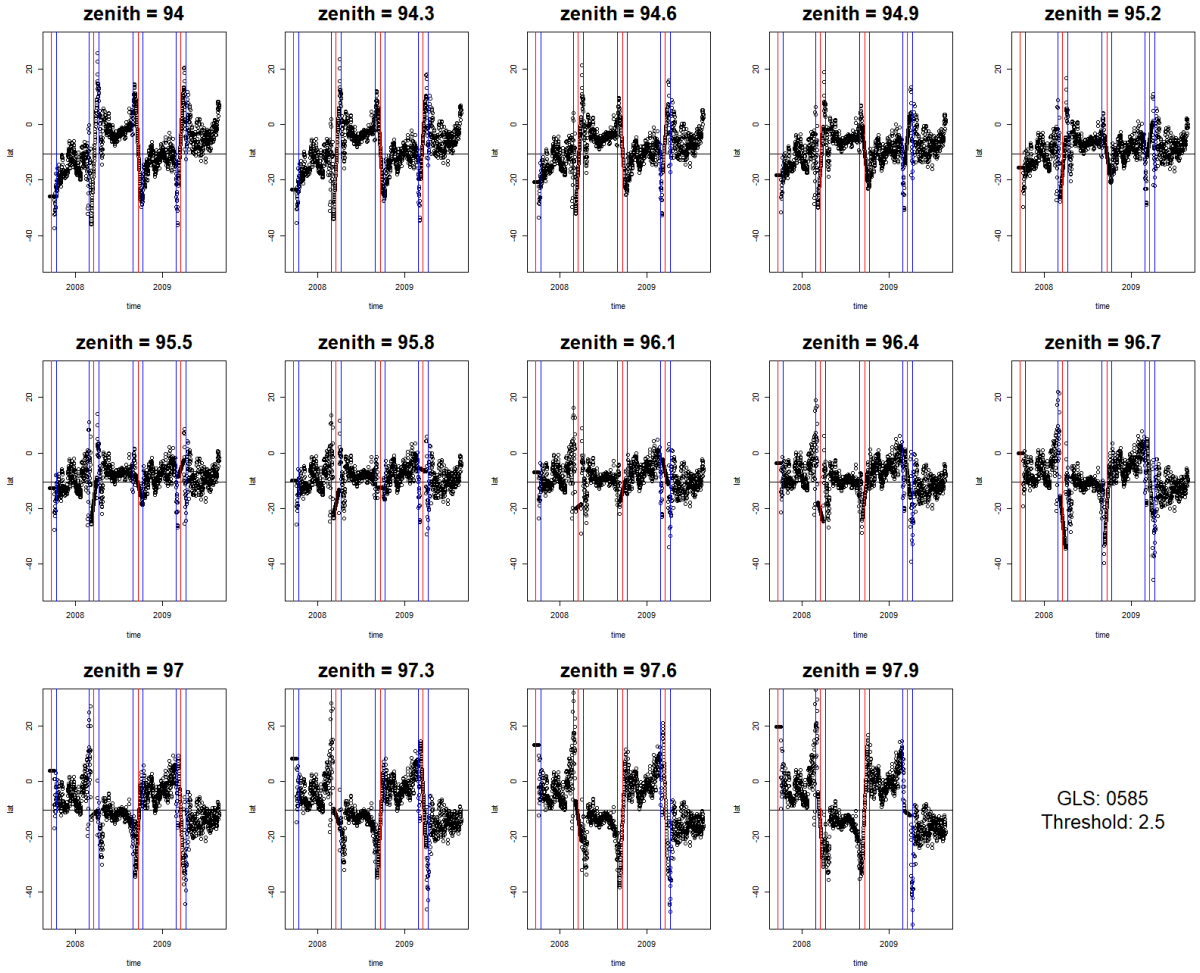

Figure S9. Latitude of location estimates (simple threshold method) over time at different zenith angles for the full deployment period of an example GLS. Red lines: equinoxes; blue lines: equinox ± 21 days; black line: latitude of Christmas Island.

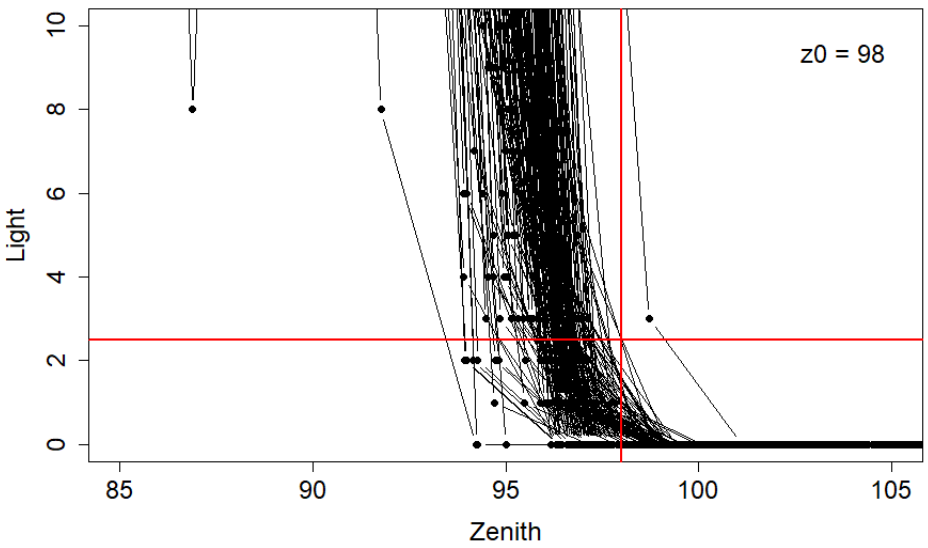

Figure S10. Zenith angle observed on Christmas Island at the time of the GLS light records for the on-bird calibration period of an example GLS. Red horizontal line: threshold; red vertical line: zenith 0 deviation (z0). The outlier twilight to the right is not considered for the determination of z0 as the bird was most likely not on Christmas Island at the time.

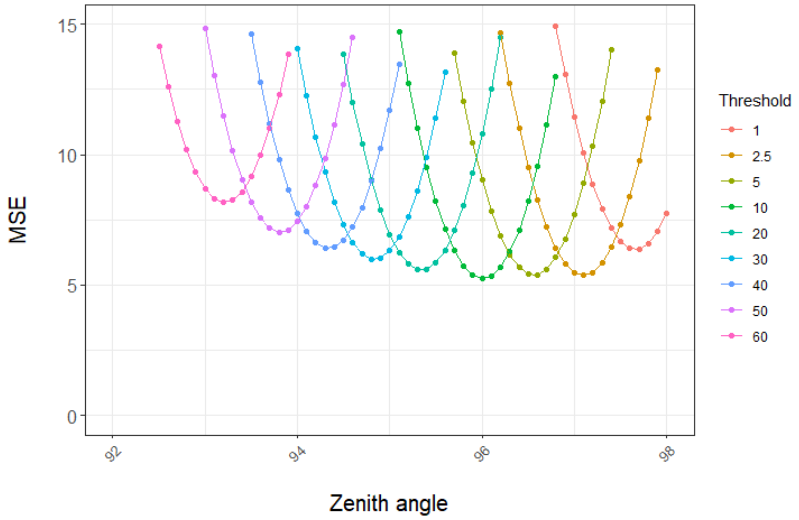

Figure S11. Mean squared error (MSE) of latitude difference between location estimates and Christmas Island for the stationary GLS.

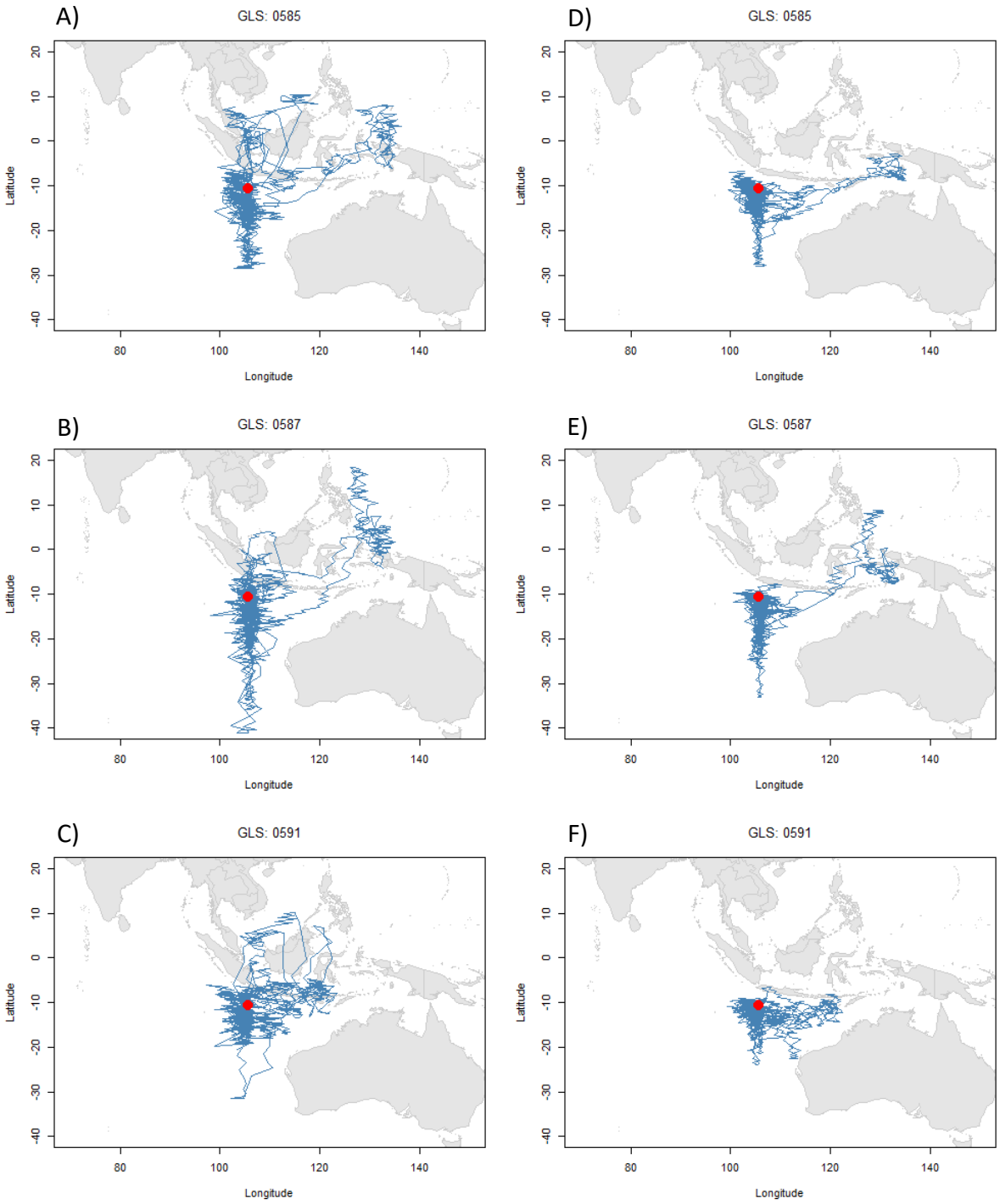

Figure S12. Tracks of location estimates for the three deployed Mk4 GLS for birds that undertook a migration with locations refined using (A,B,C) roof-top calibration values from the stationary Mk4 GLS left 10 months on Christmas Island, and (D,E,F) calibration values from individual GLS on-bird calibration. Red dot: Christmas Island.

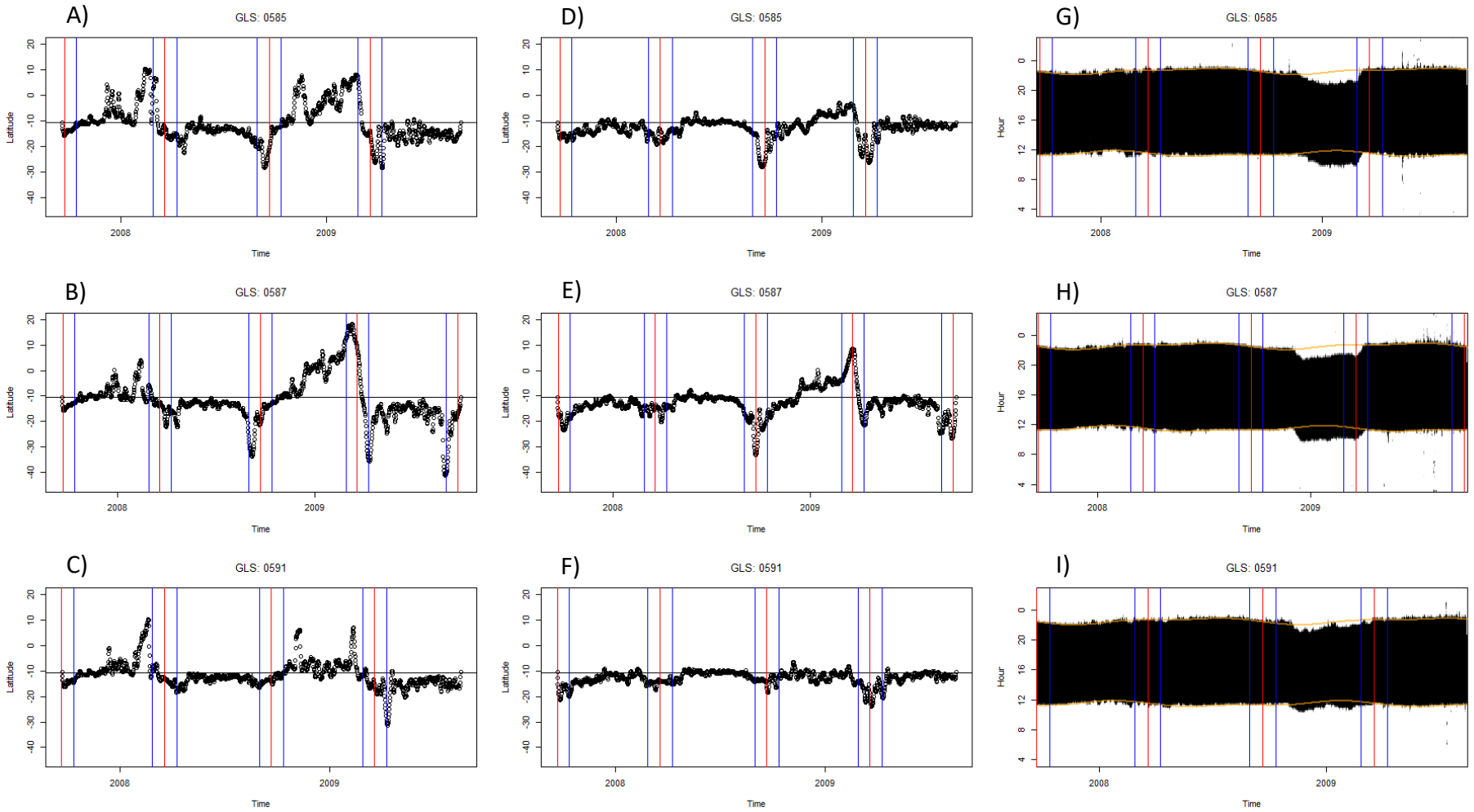

Figure S13. Latitude of location estimates over time for the three deployed Mk4 GLS for birds that undertook a migration with locations refined using (A,B,C) roof-top calibration values from the stationary Mk4 GLS left 10 months on Christmas Island, and (D,E,F) calibration values from individual GLS on-bird calibration. (G,H,I) Light data recorded by the three GLS compared to expected twilights at Christmas Island (orange lines). Red lines: equinoxes; blue lines: equinox ± 21 days. Horizontal black line (A to F): latitude of Christmas Island.

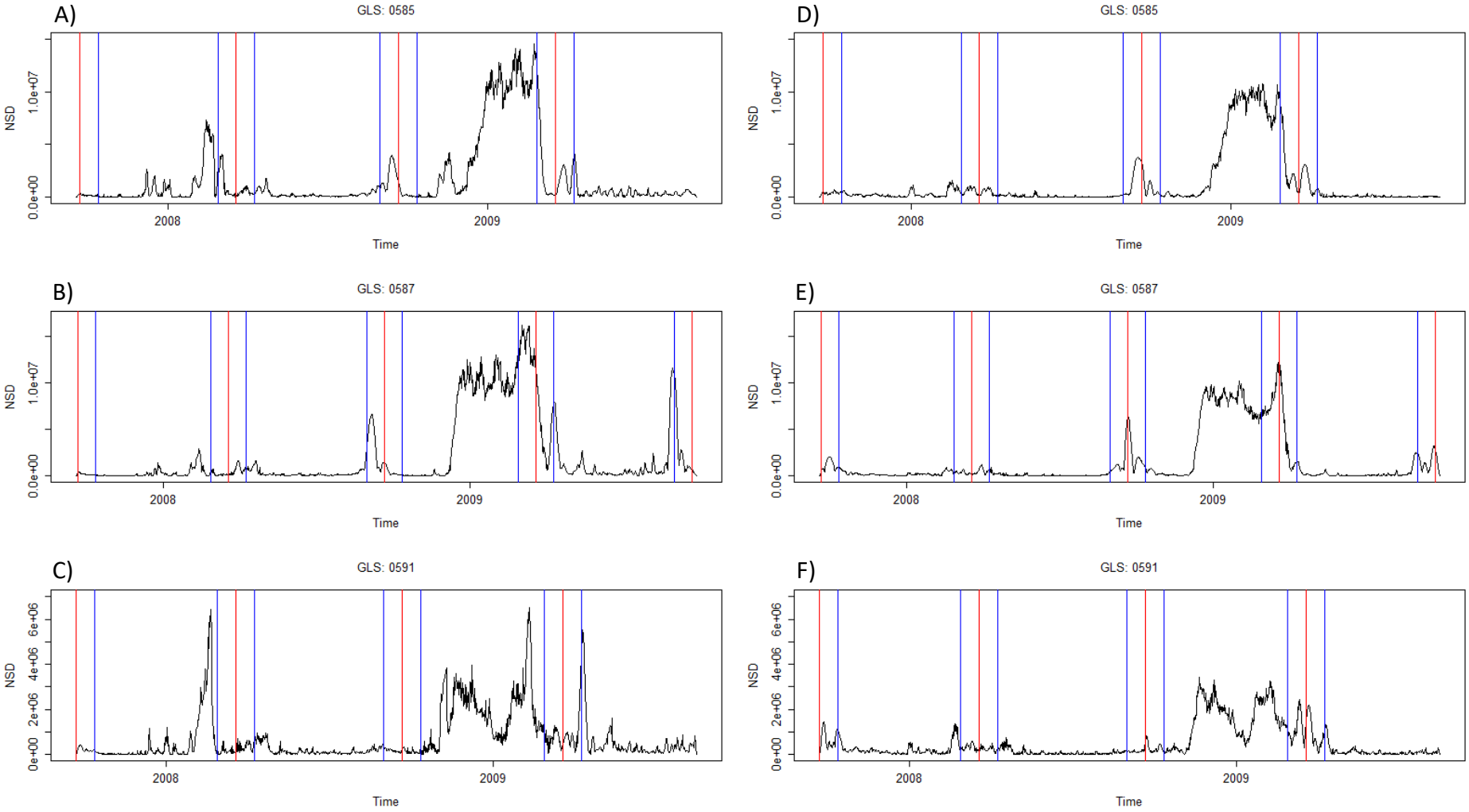

Figure S14. Net squared displacement (NSD) for the three deployed Mk4 GLS for birds that undertook a migration with locations refined using (A,B,C) roof-top calibration values from the stationary Mk4 GLS left 10 months on Christmas Island, and (D,E,F) calibration values from individual GLS on-bird calibration. Red lines: equinoxes; blue lines: equinox ± 21 days.

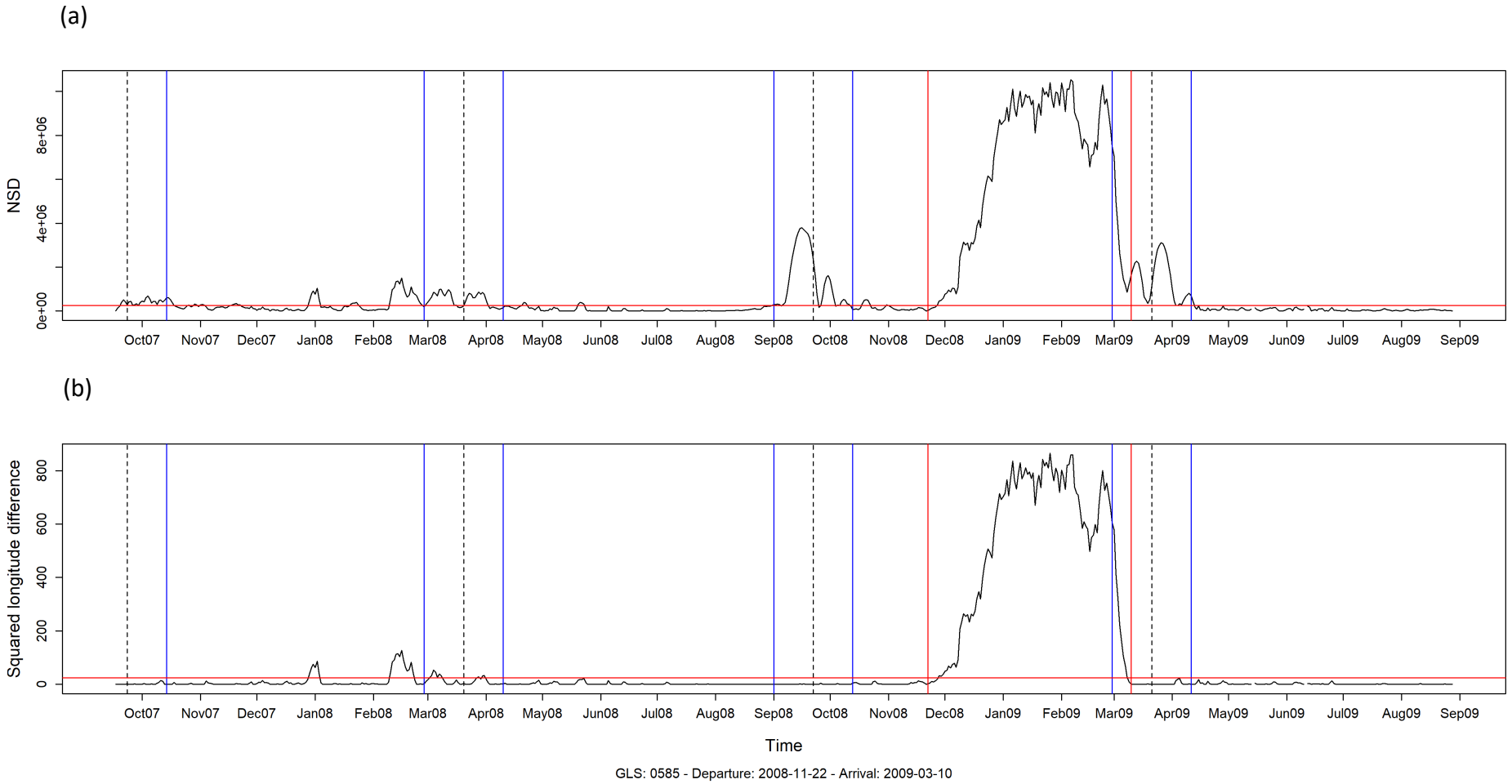

Figure S15. Determination of non-breeding migration departure and return dates using (a) net squared displacement (NSD), and (b) squared longitude difference for an example GLS. Dashed lines: equinoxes; blue lines: equinox ± 21 days; red horizontal lines: 500 km threshold; red vertical lines: boundaries of defined migration period.

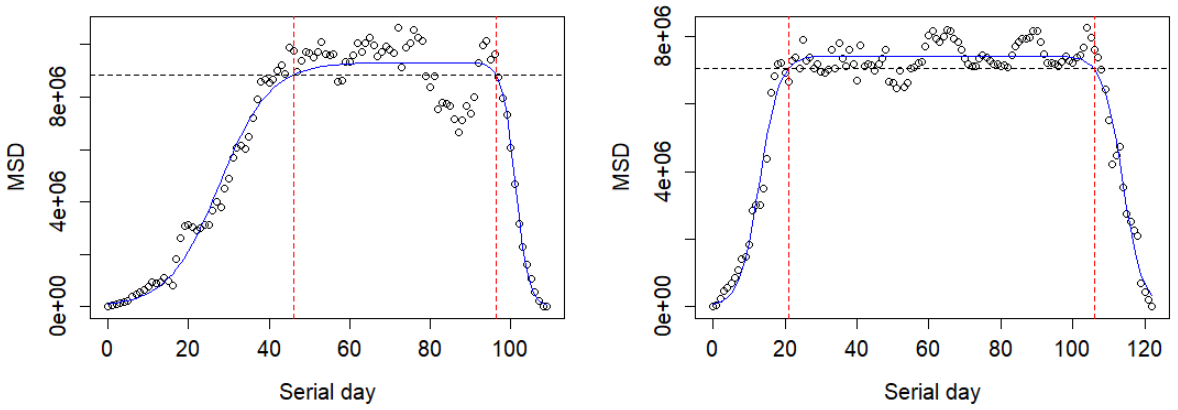

Figure S16. Mean Squared Displacement (MSD) of location estimates during the non-breeding migration for two example GLS, with fitted migration model (blue line) and arrival/departure from the non-breeding range (red lines). Black line: 95% of model asymptote.

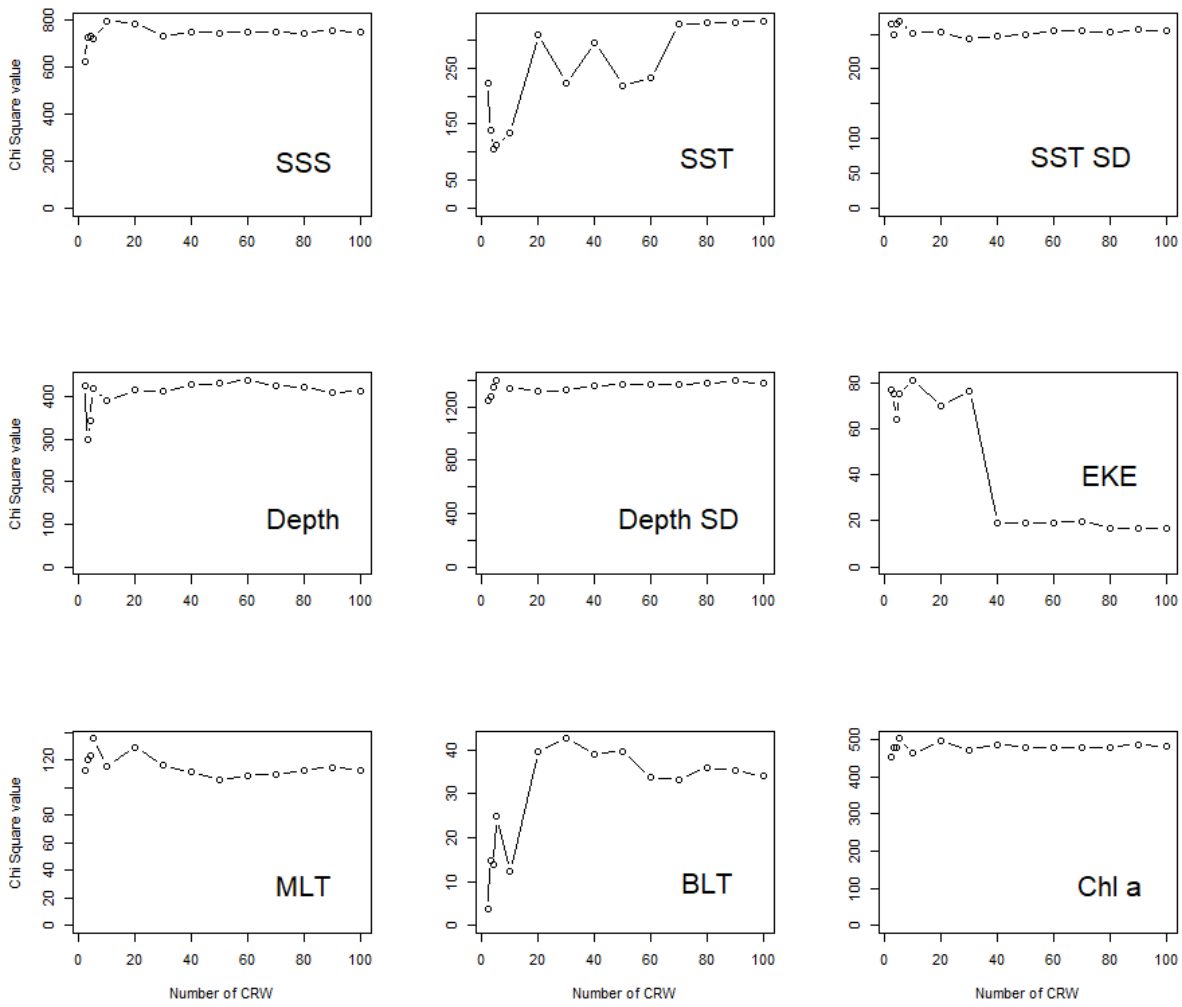

Figure S17. Chi Square values for the environmental variables with an increasing number of correlated random walks.

TABLES

Table S1. Non-breeding range distance ("NB range" in km, mean ± SD) and area of individual 50%, 95% and 99.9% utilisation distributions (10^5 km², mean ± SD). In brackets: the number of full migrations used for the calculation of the non-breeding range distance (see 'methods').

Group	n_{full}	NB range	50% UD area	95% UD area	99.9% UD area
Female	13(11)	2,464 ± 814	5.71 ± 1.86	25.90 ± 7.26	50.84 ± 12.39
Male	14	2,584 ± 386	5.28 ± 1.88	28.44 ± 8.05	56.98 ± 13.65
Failed	16(15)	2,656 ± 443	5.45 ± 1.98	27.34 ± 6.44	54.23 ± 10.68
Successful	7(6)	2,527 ± 685	6.05 ± 1.05	27.08 ± 6.56	52.71 ± 11.25
Unknown	4	2,071 ± 907	4.62 ± 2.47	26.94 ± 14.56	55.50 ± 26.00
Female x Failed	6(5)	2,679 ± 647	5.95 ± 2.10	26.32 ± 7.30	51.27 ± 12.87
Female x Successful	5(4)	2,631 ± 731	6.43 ± 0.97	28.18 ± 7.14	54.32 ± 11.88
Female x Unknown	2	1,595 ± 1,221	3.17 ± 0.07	18.92 ± 6.15	40.84 ± 13.74
Male x Failed	10	2,644 ± 346	5.15 ± 1.95	27.95 ± 6.20	56.01 ± 9.41
Male x Successful	2	2,321 ± 783	5.10 ± 0.53	24.32 ± 5.76	48.70 ± 12.23
Male x Unknown	2	2,548 ± 261	6.08 ± 3.15	34.96 ± 18.47	70.16 ± 31.31
Total	27(25)	2,531 ± 600	5.48 ± 1.85	27.21 ± 7.64	54.03 ± 13.18

Table S2. Total duration of the non-breeding migration and duration of the phenophases (days, mean ± SD). Out = outbound migration, NB = non-breeding range residency; Back = return migration. In brackets: the number of complete migrations when it differs from the total number of migrations ($n_{migrations}$). The total duration and the durations at non-breeding area and of the return migration were calculated from the complete migrations only.

Group	$n_{migrations}$	n_{birds}	Total	Out	NB	Back
Female	13	10	114.69 ± 32.85	42.77 ± 20.77	47.46 ± 39.23	24.46 ± 14.69
Male	16(14)	12	127.43 ± 16.54	24.25 ± 11.32	81.29 ± 33.49	22.29 ± 19.91
Failed	18(16)	16	116.06 ± 20.09	32.39 ± 17.28	62.00 ± 38.68	21.00 ± 12.51
Successful	7	7	125.14 ± 29.33	39.71 ± 24.19	56.29 ± 31.57	29.14 ± 27.63
Unknown	4	4	135.50 ± 40.98	20.75 ± 4.11	92.25 ± 53.85	22.50 ± 13.20
Female x Failed	6	6	106.67 ± 27.50	45.00 ± 19.87	36.67 ± 39.99	25.00 ± 14.95
Female x Successful	5	5	123.60 ± 35.71	49.20 ± 21.90	54.00 ± 33.67	20.40 ± 17.27
Female x Unknown	2	2	116.50 ± 57.28	20.00 ± 2.83	63.50 ± 67.18	33.00 ± 7.07
Male x Failed	12(10)	10	121.70 ± 12.60	26.08 ± 12.32	77.20 ± 30.34	18.60 ± 10.93
Male x Successful	2	2	129.00 ± 4.24	16.00 ± 4.24	62.00 ± 36.77	51.00 ± 45.25
Male x Unknown	2	2	154.50 ± 17.68	21.50 ± 6.36	121.00 ± 29.70	12.00 ± 5.66
Total	29(27)	22	121.3 ± 26.02	32.55 ± 18.47	65.00 ± 39.60	23.33 ± 17.29

Table S3. Timing of the phenophases (day of the year, mean ± SD; adjusted for the start and end of the outbound migration, i.e., 365 added to day of year for dates in first half of the year). Out: outbound migration; Back = return migration. In brackets: the number of complete migrations when it differs from the total number of migrations ($n_{migrations}$). The start and end of the return migration were only calculated for complete migrations.

Group	$n_{migrations}$	n_{birds}	Start Out	End Out	Start Back	End Back
Female	13	10	342.23 ± 28.55	384.62 ± 36.88	66.92 ± 30.05	91.46 ± 27.46
Male	16(14)	12	338.50 ± 23.22	362.69 ± 24.40	78.21 ± 35.27	100.57 ± 21.93
Failed	18(16)	16	349.17 ± 25.91	381.39 ± 32.15	80.12 ± 32.40	101.19 ± 26.06
Successful	7	7	322.43 ± 18.46	361.71 ± 32.75	52.57 ± 24.51	81.86 ± 14.96
Unknown	4	4	330.75 ± 12.87	351.50 ± 15.15	78.75 ± 39.36	101.25 ± 28.25
Female x Failed	6	6	362.00 ± 24.14	406.67 ± 31.95	78.33 ± 36.45	103.33 ± 30.24
Female x Successful	5	5	320.40 ± 21.37	369.00 ± 36.20	57.60 ± 10.31	78.20 ± 16.27
Female x Unknown	2	2	337.50 ± 16.26	357.50 ± 19.09	56.00 ± 48.08	89.00 ± 41.01
Male x Failed	12(10)	10	342.75 ± 25.26	368.75 ± 24.72	81.20 ± 31.76	99.90 ± 24.88
Male x Successful	2	2	327.50 ± 12.02	343.50 ± 16.26	40.00 ± 52.33	91.00 ± 7.07
Male x Unknown	2	2	324.00 ± 7.07	345.50 ± 13.44	101.50 ± 16.26	113.50 ± 10.61
Total	29(27)	22	340.17 ± 25.33	372.52 ± 32.02	72.78 ± 32.74	96.19 ± 24.7

Table S4. Known observations of Abbott's boobies more than 500 km off Christmas Island by bird/marine wildlife boat tour companies (C) and in published articles (A).

Date	Female	Male/Juvenile	Unknown	Latitude	Longitude	Country/Territory	Locality	Source
07 Jan 1985			1	-4.82	125.75	Indonesia		Smeenk 1985 (A)
18 Jan 1985			4	-2.67	127.87	Indonesia		Smeenk 1985 (A)
23 Jan 1985			4	-4.48	132.98	Indonesia		Smeenk 1985 (A)
25 Jan 1985			6	-7.81	132.41	Indonesia		Smeenk 1985 (A)
19 Feb 1985			3	-5.28	133.98	Indonesia	Between Aru and Kai Islands	Cadée 1989 (A)
02 May 1994	1			-5.13	132.28	Indonesia	Northwest of the Tayandu Islands	van Balen 1996 (A)
04 May 1994		1		-3.55	129.72	Indonesia	Between Seram and Saparua	van Balen 1996 (A)
16 Dec 1999		1		-18.33	122.05	Australia	Eco Beach, Western Australia	Hassell & Boyle 2000 (A)
17 Apr 2007	1			14.16	145.28	Northern Mariana Islands	Rota Island	Pratt et al. 2009 (A)
29 Nov 2010	1			14.15312	145.268665	Northern Mariana Islands	Rota Island	Birdquest (C)
06 Oct 2014			1	2.167	73.317	Maldives	Between Thaa and Laamu Atolls	Anderson et al. 2016 (A)
04 Nov 2014			1	-8.35	119.20	Indonesia	Selat Sape (west of Komodo)	Whale and Dolphin Company (C)
13 Oct 2015			1	-8.02	117.54	Indonesia	Near Satonda (north of Sumbawa)	Whale and Dolphin Company (C)
15 Mar 2017	1			-1.25510	129.3002	Indonesia	Northwest of Kofiau Island	Birdtour Asia (C)
07 Mar 2017			1	-0.490202	130.092892	Indonesia	Dampier Strait	Wildiaries (C)
24 Oct 2018			1	-1.38743	127.9505	Indonesia	Off Obi Island	Rockjumper (C)
15 Sep 2019			1	-8.15	117.16	Indonesia	Northwest of Sumbawa	Whale and Dolphin Company (C)
19 Sep 2023			1	-8.2967	120.7783	Indonesia	Off Northwest Flores	Whale and Dolphin Company (C)

Table S5. Proportion of time spent in contact with water (median; in brackets IQR and range). Parameters were first calculated per individual then averaged across individuals.

Group	n_{tracks}	n_{birds}	n_{data}	Dawn	Daylight	Dusk	Night
Female	9	8	978	0.14 (0.09 - 0.24; 0.00 - 0.83)	0.18 (0.11 - 0.29; 0.01 - 0.59)	0.14 (0.06 - 0.26; 0.00 - 0.82)	0.18 (0.10 - 0.37; 0.00 - 0.89)
Male	10	9	984	0.03 (0.00 - 0.23; 0.00 - 0.97)	0.13 (0.06 - 0.23; 0.01 - 0.58)	0.10 (0.04 - 0.25; 0.00 - 0.85)	0.13 (0.03 - 0.34; 0.00 - 0.98)
Failed	13	12	1279	0.11 (0.07 - 0.28; 0.00 - 0.97)	0.17 (0.10 - 0.27; 0.01 - 0.63)	0.16 (0.08 - 0.30; 0.00 - 0.89)	0.20 (0.09 - 0.39; 0.00 - 0.99)
Successful	6	6	683	0.02 (0.00 - 0.11; 0.00 - 0.75)	0.12 (0.05 - 0.24; 0.01 - 0.50)	0.03 (0.00 - 0.15; 0.00 - 0.72)	0.06 (0.01 - 0.29; 0.00 - 0.82)
Female x Failed	5	5	543	0.23 (0.17 - 0.33; 0.00 - 0.98)	0.22 (0.15 - 0.32; 0.01 - 0.66)	0.22 (0.11 - 0.33; 0.00 - 0.86)	0.26 (0.17 - 0.41; 0.00 - 0.98)
Female x Successful	4	4	435	0.02 (0.00 - 0.12; 0.00 - 0.64)	0.13 (0.06 - 0.26; 0.01 - 0.52)	0.04 (0.00 - 0.17; 0.00 - 0.78)	0.08 (0.01 - 0.33; 0.00 - 0.77)
Male x Failed	8	7	736	0.04 (0.00 - 0.26; 0.00 - 0.96)	0.14 (0.07 - 0.24; 0.01 - 0.61)	0.12 (0.06 - 0.28; 0.00 - 0.91)	0.15 (0.04 - 0.37; 0.00 - 1.00)
Male x Successful	2	2	248	0.01 (0.00 - 0.10; 0.00 - 0.97)	0.08 (0.04 - 0.19; 0.01 - 0.47)	0.01 (0.00 - 0.10; 0.00 - 0.61)	0.02 (0.00 - 0.21; 0.00 - 0.90)
Total	19	18	1962	0.08 (0.05 - 0.23; 0.00 - 0.90)	0.15 (0.08 - 0.26; 0.01 - 0.59)	0.12 (0.05 - 0.52; 0.00 - 0.84)	0.15 (0.07 - 0.36; 0.00 - 0.93)

LITERATURE CITED

Anderson RC, Bray N, Maher M (2016) First records of three seabirds for the Maldives. BirdingASIA 26:129-131

Biotrack Ltd. (2013) M-Series Geolocator User Manual v11. Biotrack Limited, Wareham, Dorset, UK

Börger L (2021) Core Area. In: Vonk J, Shackelford T (eds) Encyclopedia of Animal Cognition and Behavior. Springer, Cham, p 1-3

Börger L, Fryxell J (2012) Quantifying individual differences in dispersal using net squared displacement. In: Clobert J, Baguette M, Benton TG, Bullock JM (eds) Dispersal Ecology and Evolution. Oxford Scholarship Online, p 222-230

Bråthen VS, Moe B, Amélineau F, Ekker M and others (2021) An automated procedure (v2.0) to obtain positions from light-level geolocators in large-scale tracking of seabirds. A method description for the SEATRACK project. NINA Report 1893. Norwegian Institute for Nature Research. https://hdl.handle.net/11250/2735757 accessed 18 Nov 2021

Bunnefeld N, Borger L, van Moorter B, Rolandsen CM, Dettki H, Solberg EJ, Ericsson G (2011) A model-driven approach to quantify migration patterns: individual, regional and yearly differences. J Anim Ecol 80:466-476

Cadée GC (1989) Seabirds in the Banda Sea in February/March 1985. Marine Research in Indonesia 27:19-34

Calenge C (2006) The package adehabitat for the R software: a tool for the analysis of space and habitat use by animals. Ecological Modelling 197:516-519

Clay TA, Phillips RA, Manica A, Jackson HA, Brooke M (2017) Escaping the oligotrophic gyre? The year-round movements, foraging behaviour and habitat preferences of Murphy's petrels. Marine Ecology Progress Series 579:139-155

Fieberg J (2007) Kernel density estimators of home range: smoothing and the autocorrelation red herring. Ecology 88:1059-1066

Fieberg J, Börger L (2012) Could you please phrase "home range" as a question? Journal of Mammalogy 93:890-902

Fromant A, Bost C-A, Bustamante P, Carravieri A and others (2020) Temporal and spatial differences in the post-breeding behaviour of a ubiquitous Southern Hemisphere seabird, the common diving petrel. Royal Society Open Science 7:200670

Halpin LR, Ross JD, Ramos R, Mott R and others (2021) Double-tagging scores of seabirds reveals that light-level geolocator accuracy is limited by species idiosyncrasies and equatorial solar profiles. Methods in Ecology and Evolution 12:2243-2255

Hassell CJ, Boyle AN (2000) Abbott's Booby: First record for mainland Australia. Australian Bird Watcher 18:255–258

Hennicke JC, Weimerskirch H (2014) Coping with variable and oligotrophic tropical waters: foraging behaviour and flexibility of the Abbott's booby *Papasula abbotti*. Marine Ecology Progress Series 499:259-273

Hennicke JC, Weimerskirch H (2014) Foraging movements of Abbott's Boobies during early chick-rearing and implications for a marine Important Bird Area in Christmas Island waters. Raffles Bulletin of Zoology 30:60-64

Hill RD, Braun MJ (2001) Geolocation by light level – the next step: latitude. In: Sibert JR, Nielsen J (eds) Electronic Tagging and Tracking in Marine Fisheries. Kluwer Academic Publishers, The Netherlands

Hines WGS, O'Hara Hines RJ, Pond B, Obbard ME (2005) Allowing for redundancy and environmental effects in estimates of home range utilization distributions. Environmetrics 16:33-50

Hipfner JM, Prill MM, Studholme KR, Domalik AD and others (2020) Geolocator tagging links distributions in the non-breeding season to population genetic structure in a sentinel North Pacific seabird. PLoS ONE 15:e0240056

Horne JS, Fieberg J, Börger L, Rachlow JL, Calabrese JM, Fleming CH (2020) Animal Home Ranges. In: Murray DL, Sandercock BK (eds) Population Ecology in Practice. John Wiley & Sons Ltd, p 315-332

Lascelles BG, Taylor PR, Miller MGR, Dias MP and others (2016) Applying global criteria to tracking data to define important areas for marine conservation. Diversity and Distributions 22:422-431

Lisovski S, Bauer S, Briedis M, Davidson SC and others (2019) Light-level geolocator analyses: A user's guide. J Anim Ecol 89:221-236

Lisovski S, Hahn S, Hodgson D (2012) GeoLight - processing and analysing light-based geolocator data in R. Methods in Ecology and Evolution 3:1055-1059

Lisovski S, Hewson CM, Klaassen RHG, Korner-Nievergelt F, Kristensen MW, Hahn S (2012) Geolocation by light: accuracy and precision affected by environmental factors. Methods in Ecology and Evolution 3:603-612

Merkel B, Phillips RA, Descamps S, Yoccoz NG, Moe B, Strom H (2016) A probabilistic algorithm to process geolocation data. Mov Ecol 4:26

Morris-Pocock JA, Hennicke JC, Friesen VL (2012) Effects of long-term isolation on genetic variation and within-island population genetic structure in Christmas Island (Indian Ocean) seabirds. Conservation Genetics 13:1469-1481

Nelson JB, Powell DA (1986) The breeding ecology of Abbott's Booby. Emu 86:33–46

Phillips RA, Silk JRD, Croxall JP, Afanasyev V, Briggs DR (2004) Accuracy of geolocation estimates for flying seabirds. Marine Ecology Progress Series 266:265-272

Pinheiro J, Bates D, DebRoy S, Sarkar D, R Core Team (2021) nlme: Linear and Nonlinear Mixed Effects Models. R package version 3.1-152

Pratt HD, Retter MLP, Chapman D, Michael Ord W, Pisano P (2009) An Abbott's Booby *Papasula abbotti* on Rota, Mariana Islands: First historical record for the Pacific Ocean. Bulletin of the British Ornithologists' Club 129:87-91

Quaglietta L, Porto M (2023) SiMRiv: Individual-Based, Spatially-Explicit Simulation and Analysis of Multi-State Movements in River Networks and Heterogeneous Landscapes. R package version 1.0.6

Smeenk C (1985) Whales and seabirds. In: Postma H, Rommets J (eds) Progress Report Snellius II Expedition. Theme II Ventilation of deep sea basins, cruise MV Tyro, Janurary 4 – February 6 1985. KNAW/LIPI, p 1-26

Sumner MD, Wotherspoon SJ, Hindell MA (2009) Bayesian estimation of animal movement from archival and satellite tags. PLoS One 4:e7324

van Balen S (1996) Note on observations of Abbott's Booby in the Banda Sea. Kukila 8:145-146

Wotherspoon S, Sumner MD, Lisovski S (2021) SGAT: Solar/Satellite Geolocation for Animal Tracking. R package version 0.1.3. https://rdrr.io/github/SWotherspoon/SGAT/

Yorkston HD, Green PT (1997) The breeding distribution and status of Abbott's booby (Sulidae: *Papasula abbotti*) on Christmas Island, Indian Ocean. Biological Conservation 79:293-301

Žydelis R, Lewison RL, Shaffer SA, Moore JE, Boustany AM, Roberts JJ, Sims M, Dunn DC, Best BD, Tremblay Y, Kappes MA, Halpin PN, Costa DP, Crowder LB (2011) Dynamic habitat models: using telemetry data to project fisheries bycatch. Proc Biol Sci 278:3191–200